JACS
JOURNAL OF THE AMERICAN CHEMICAL SOCIETY

COMMUNICATION

pubs.acs.org/JACS

Electrochemical Unzipping of Multi-walled Carbon Nanotubes for Facile Synthesis of High-Quality Graphene Nanoribbons

Dhanraj B. Shinde,[†] Joyashish Debgupta,[†] Ajay Kushwaha,[§] Mohammed Aslam,[§] and Vijayamohanan K. Pillai*[,†,‡]

[†]Physical and Materials Chemistry Division, National Chemical Laboratory, Pune 411 008, India

[‡]Central Electrochemical Research Institute, Chennai, Karaikudi 630 006, India

[§]Indian Institute of Technology, Mumbai 400 076, India

Supporting Information

ABSTRACT: Here we report a remarkable transformation of carbon nanotubes (CNTs) to nanoribbons composed of a few layers of graphene by a two-step electrochemical approach. This consists of the oxidation of CNTs at controlled potential, followed by reduction to form graphene nanoribbons (GNRs) having smooth edges and fewer defects, as evidenced by multiple characterization techniques, including Raman spectroscopy, atomic force microscopy, and transmission electron microscopy. This type of "unzipping" of CNTs (single-walled, multi-walled) in the presence of an interfacial electric field provides unique advantages with respect to the orientation of CNTs, which might make possible the production of GNRs with controlled widths and fewer defects.

Graphene is a one-atom-thick planar sheet of sp^2-bonded carbon atoms, densely packed in a honeycomb lattice, that has attracted tremendous attention for both fundamental research related to the exotic behavior of electrons in two-dimensional systems and also possible applications in nanoelectronics, supercapacitors, solar cells, and hydrogen storage.[1,2] Graphene exhibits many exciting properties, such as room-temperature quantum Hall effect,[3] long-range ballistic transport with ~10 times higher electron mobility than in Si,[4] availability of charge carriers that behave as mass-less relativistic quasi particles (Dirac fermions),[5] and quantum confinement resulting in finite band gap and Coulomb blockade effects,[6] which could be useful for making many novel electronic devices. However, in order to fully realize these properties and applications, consistent, reliable, and inexpensive methods for growing high-quality graphene layers in excellent yields are crucial, as the existence of residual defects will heavily impact their electronic properties, despite their expected insensitivity to impurity scattering. Unfortunately, many of the existing methods of graphene preparation have several major limitations. For example, preparations by mechanical cleavage,[7] silicon carbide sublimation,[8] solvothermal synthesis,[9] chemical vapor deposition,[10] and plasma etching[11] suffer from limitations such as poor quality and yield of graphene ribbons, formation of over-oxidized and defective nanoribbons, substrate-dependent behavior, and the difficulty of controlling both layer thickness and edge smoothness in a predictable manner. Hence, accurate control of the quality of graphene layers along with their preparation in good yields is a daunting task.

One of the more successful approaches, to date, for converting carbon nanotubes (CNTs) to graphene is the recently reported longitudinal unzipping,[12] using a mixture of potassium permanganate and concentrated sulfuric acid, facilitating a large-scale preparation of graphene nanoribbons (GNRs). However, this method has several problems, primarily related to the selection of strong oxidizing agents. The choice to use chemical oxidation itself has serious issues, like over-oxidation of edges that will create defect sites which hamper the electronic properties of graphene. More significantly, electron mobility and conductivity diminish with this treatment, and there is a possibility of evolution of explosive gases. In addition, the use of strong reducing agents might pose difficulties in controlling the layer thickness of graphene ribbons, along with disposal concerns. In comparison, electrochemical oxidation can ensure accurate control of the degree and sites of oxidation (especially with controlled potential techniques) under ambient conditions; hence, this method is capable of providing more precise unzipping of nanotubes in comparison with chemical and plasma-based approaches. Since CNTs are graphene sheets seamlessly rolled into concentric tubes, from a geometrical perspective it may be possible to transform CNTs to graphene by a longitudinal cutting of all C−C bonds along the tube axis. Many computational approaches[14] have recently attempted to reveal the exact geometric steps as well as the energetics of the process of unzipping, despite ardent challenges, and all these suggest that it is possible, in principle, to open tubes by applying an appropriate electric field.

Here we report an unprecedented method for transforming CNTs to GNRs by using an electrochemical approach, with the unique advantage that it allows controlling the graphene layer thickness and orientation. The electrochemical approach is an effective way to modify electronic states by modulating the electric field (chemical potential) to change the Fermi level of the electrode materials.[13] An interfacial electric field is expected to orient the CNTs in our method, and hence longitudinal unzipping is more likely with possible C−C cleavage initiated at topological defects having enough strain, rather than a random breakdown in chemical methods. Unfortunately, large graphene sheets cannot be made in this way, since the size of the graphene

Received: October 1, 2010
Published: March 09, 2011

dx.doi.org/10.1021/ja1101739 | J. Am. Chem. Soc. 2011, 133, 4168–4171

Scheme 1. Diagrammatic Representation of the Electrochemical Transformation of GNRs from MWCNTs: (a) Pristine MWCNT; (b) MWCNT Deposited on Glassy Carbon Electrode after Oxidation To Generate Functional Groups on Edges under Controlled Potential So That It Gets Broken; (c) Electrochemical and (d) Chemical Reduction to Graphene Layers

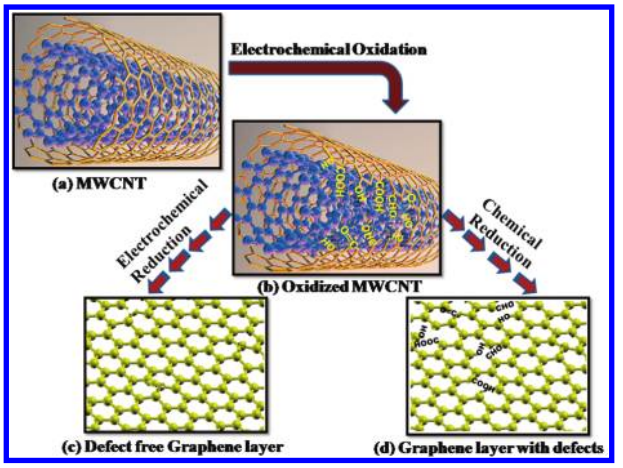

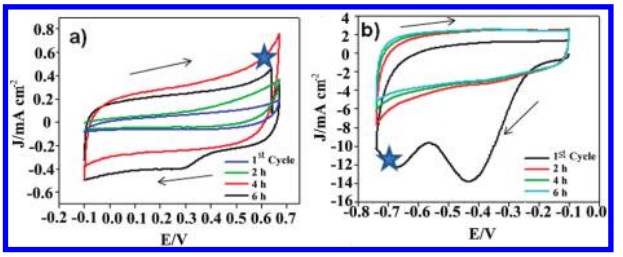

Figure 1. (a) Cyclic voltammograms (oxidation) of MWCNTs in the potential window from 0.1 to 0.7 V vs MMS in 0.5 M H_2SO_4 using glassy carbon electrode at 100 mV/s scan rate. (b) Cyclic voltammograms (reduction) of MWCNTs in the potential window from −0.1 to −0.75 V vs MMS in 0.5 M H_2SO_4 at 100 mV/s scan rate. Regions marked with a star indicate the potentials at which the CNTs have been selectively oxidized or reduced.

is limited by the diameter of the multi-walled carbon nanotubes (MWCNTs).

Scheme 1 represents our two-step process for the electrochemical transformation of MWCNTs to graphene layers. The first step involves applying a typical anodic potential of 0.70 V vs mercury|mercury(I) sulfate (MMS) electrode to the MWCNT working electrode in 0.5 M H_2SO_4, where the applied electric field initiates the breaking of sp^2 carbon bonds, perhaps at the tip of the MWCNT. This continues in the longitudinal direction, as evidenced by subtle changes in the voltammogram (Figure 1). Broken MWCNTs along a straight line are stretched farther away by the tension in the curved surface, which could result in the remarkable transformation into graphene oxide layers.[14] This speculative mechanism, however, needs more experimental evidence to provide a complete understanding of the intermediates formed after C−C cleavage. We have achieved the same electrochemical unzipping process in single-walled carbon nanotubes (SWCNTs), to produce narrow nanoribbons, but their subsequent disentanglement appears to be more difficult (Figure S7).

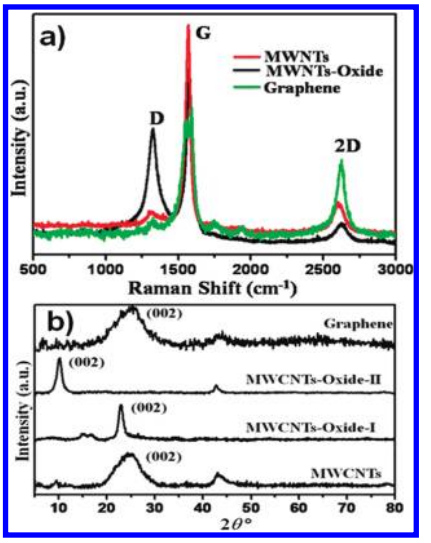

Figure 2. Comparisons of (a) Raman spectra and (b) powder XRD patterns for MWCNTs, oxidized MWCNTs, and graphene.

During the anodic scan from the open-circuit potential 0.1 to 0.7 V, there is no clear peak. More significantly, the increase in non-faradic current with cycle number and time suggests subtle morphological changes, including that of the area. By keeping the potential at 0.7 V for 6 h, the oxidation of MWCNTs generates an enormous number of oxygen functionalities, and interestingly at the end, the open-circuit potential also increases by 60 mV, clearly revealing the formation of many of these groups. This complete oxidation of MWCNTs in 6 h is also supported by a comparison of the Fourier transform infrared (FT-IR) spectra of pristine, oxidized, and subsequently reduced samples, showing a characteristic stretching frequency at 1720 cm^{-1} corresponding to the carbonyl group for oxidized MWCNTs and also decreased conductivity values, as shown in Figures S3 and S4. Subsequent reduction of these oxidized MWCNTs in the potential range from −0.1 to −0.75 V shows a large cathodic current at −0.43 V for MWCNTs, indicating rapid kinetics compared to the oxidation in the previous step. This large reduction current is ascribed to the removal of surface oxygen groups. There could be intrinsic resistivity changes in the materials as a function of cycle number, and also interestingly, a change in double-layer capacitance (from 40 to 10 μF/cm^2) when oxidized MWCNTs are completely converted to GNRs, reflecting more of the double-layer capacitance and adsorption-induced pseudo-capacitance. A significant improvement in electronic conductivity after GNR formation also supports this (Figure S4).

Raman spectroscopy is a powerful and nondestructive tool to distinguish between different types of ordered and disordered bonding environments of sp^2- and sp^3-hybridized carbon. Normally in carbon nanostructures the G band is assigned to the E_{2g} phonon of sp^2 carbon atoms, while D band intensity corresponds to the extent of defects.[15] In Figure 2a, the intensity of the D band at 1329 cm^{-1} of MWCNTs increases substantially, indicating a decrease in the size of in-plane sp^2 domains due to oxidation. As seen in the case of pristine MWCNTs, the intensity of the D band is less, suggesting excellent quality of the starting materials.[11] After the electrochemical oxidation, the intensity of the D band is considerably enhanced, along with a concomitant decrease in the intensity of the G band, clearly revealing that the oxidation has been completed.[16] Interestingly, by applying controlled cathodic

dx.doi.org/10.1021/ja1101739 |J. Am. Chem. Soc. 2011, 133, 4168–4171

potential in the second step, the oxidized broken GNRs are converted to graphene, as confirmed by the observation of a very low intensity ratio of D/G bands. For example, after 6 h such electrochemically unzipped MWCNTs typically show a very low I_D/I_G ratio (0.11), suggesting the edges in graphene to be very sharp and defect-free. Moreover, the intensity of the 2D band is found to be 60% relative to that of the G band, which also indicates the formation of a few layers of graphene. More significantly, all these observations in Raman spectra are in excellent agreement with similar changes reported recently for chemically unzipped MWCNTs[12] and also our two-probe electronic conductivity values (Figure S4).

Figure 2b shows a comparison of powder XRD patterns of MWCNTs, oxidized MWCNTs, and graphene, which provides further valuable insights into this structural transformation, as indicated by the sensitive position of the graphitic (002) peak, corresponding to various degrees of oxidation. In comparison, pristine MWCNTs show a strong peak at 26.2°, corresponding to a *d*-spacing of 3.31 Å, whereas partially oxidized MWCNTs show an additional small peak at 14.83°, corresponding to a *d*-spacing of 5.93 Å. A shift in the (002) plane to 22.9° suggests partial oxidation of MWCNTs by holding the anodic potential at 0.7 V for 4 h. However, upon complete oxidation after 6 h, this peak is observed at 10.08°, corresponding to a *d*-spacing of 8.4 Å.[17] This value is larger than the original *d*-spacing (3.31 Å) of MWCNTs, perhaps due to the presence of intercalated water and SO_4^{2-} ions between the layers. Nevertheless, when oxidized MWCNTs are electrochemically reduced during the second step, this diffraction peak appears again at 26.6°, as in the case of chemically reduced MWCNT oxides.

Figure 3a,b shows typical AFM images of GNRs prepared from MWCNTs by the two-step electrochemical process at two different potentials, −0.75 and −0.5 V, in order to get more accurate information about the change in both height and lateral dimensions. Figure 3a reveals long ribbons (1 μm) with straight edges and widths ranging from 70 to 110 nm, revealing bilayer GNRs of thickness ranging from 1.6 to 1.9 nm. This is also confirmed by the HR-TEM images (Figure 3c,d), suggesting a complete transformation of 40−60 nm diameter MWCNTs to few-layer GNRs having more or less (70−80 nm) similar width and a few micrometers length, strikingly similar to the dimensions of high-quality graphene prepared by chemical methods. The graphene nanosheets are transparent and very stable under an electron beam.[18] The mechanism of cutting of MWCNTs along the longitudinal direction could arise because of the field direction controlling the oxidative breaking of C−C bonds at some defect sites on the sidewalls.[19] Consequently, highly aligned, narrow GNRs can be made from an array of MWCNTs by this electrochemical approach, as supported by the images in Figure 3. More importantly, analysis of all our experimental data clearly shows that this method can indeed convert the majority of the starting material to GNRs by applying a two-step potential variation (first 0.70 V anodic followed by −0.75 V cathodic, each for 6 h).

In summary, a unique electrochemical approach for the synthesis of GNRs with controlled layer thickness is reported using MWCNTs and SWCNTs. As many of the limitations of chemical unzipping are due to over-oxidation and edge defects, these could be eliminated by using controlled potential step experiments with minimum contamination. Although the electrochemical route to GNRs described here offers the advantages of tuning the orientation and controlling edges and planes along the length during the first oxidation step, some of the electronic characteristics might be affected by the adsorption of cations, anions, and solvent molecules on the defect site or due to intercalation. However, this study opens new pathways for the preparation of high-quality graphene in good yield, and there are also profound implications for certain applications like fuel cells and Li battery electrodes, where CNTs are continuously kept under an electric field.

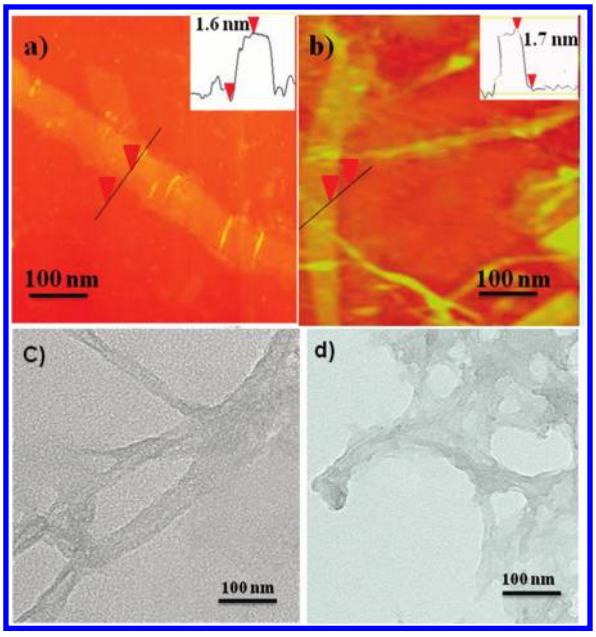

Figure 3. Typical AFM images of GNRs made from MWCNTs by the two-step electrochemical process. Top: Representative images of GNRs synthesized at (a) 0.7 and (b) 0.5 V. Bottom: TEM images of MWCNTs after two-step electrochemical treatment, revealing two to three layers of graphene sheets after (c) partial and (d) complete transformation of MWCNT.

■ ASSOCIATED CONTENT

Supporting Information. Experimental details; conductivity measurements; and XPS, FT-IR, SEM, TEM , and AFM images (Figures S1−S8). This material is available free of charge via the Internet at http://pubs.acs.org.

■ AUTHOR INFORMATION

Corresponding Author
vk.pillai@ncl.res.in

■ ACKNOWLEDGMENT

We are grateful to C Narendraraj, Ketan Bhotkar, and Premji for HR-TEM, SEM, and AFM, respectively. D.B.S. and J.D. acknowledge CSIR for financial support through the project NWP0022.

■ REFERENCES

(1) Novoselov, K. S.; Jiang, Z.; Zhang, Y.; Morozov, S. V.; Stormer, H. L.; Zeitler, U.; Maan, J. C.; Boebinger, G. S.; Kim, P.; Geim, A. K. *Science* **2007**, *315*, 1377–1378.

(2) Berger, C.; Song, Z.; Li, X.; Wu, X.; Brown, N.; Naud, C.; Mayou, D.; Li, T.; Hass, J.; Marchenkov, A. N.; Conrad, E. H.; First, P. N.; de Heer, W. A. *Science* **2006**, *312*, 1191–1195.

(3) Novoselov, K. S.; Jiang, Z.; Zhang, Y.; Morozov, S. V.; Stormer, H. L.; Zeitler, U.; Maan, J. C.; Boebinger, G. S.; Kim, P.; Geim, A. K. *Science* **2007**, *315*, 1379.
(4) Rao, C. N. R.; Sood, A. K.; Voggu, R.; Subrahmanyam, K. S. J. *Phys. Chem. Lett.* **2010**, *1*, 572–580.
(5) Novoselov, K. S.; Geim, A. K.; Morozov, S. V.; Jiang, D.; Katsnelson, M. I.; Grigorieva, I. V.; Dubonos, S. V.; Firsov, A. A. *Nature* **2005**, *438*, 197–200.
(6) Ozyilmaz, B.; Jarillo-Herrero, P.; Efetov, D.; Kim, P. *Appl. Phys. Lett.* **2007**, *91*, 192107.
(7) Li, X.; Wang, X.; Zhang, L.; Lee, S.; Dai, H. *Science* **2008**, *319*, 1229–1232.
(8) Emtsev, K. V.; Bostwick, A.; Horn, K.; Jobst, J.; Kellogg, G. L.; Ley, L.; McChesney, J. L.; Ohta, T.; Reshanov, S. A.; Rohrl, J.; Rotenberg, E.; Schmid, A. K.; Waldmann, D.; Weber, H. B.; Seyller, T. *Nat. Mater.* **2009**, *8*, 203–307.
(9) Choucair, M.; Thordarson, P.; Stride, J. *Nat. Nanotechnol.* **2009**, *4*, 669–673.
(10) Srivastav, A.; Galande, C.; Ci, L.; Song, L.; Rai, C,; Jariwala, D,; Kelly, K. F.; Ajayan, P. M. *Chem. Mater.* **2010**, *22*, 3457–3461.
(11) Jiao, L. Y.; Zhang, L.; Wang, X. R.; Diankov, G.; Dai, H. *Nature* **2009**, *458*, 877–880.
(12) Kosynkin, D. V.; Higginbotham, A. L.; Sinitskii, A.; Lomeda, J. R.; Dimiev, A.; Price, B. K.; Tour, J. M. *Nature* **2009**, *458*, 872–877.
(13) Guo, H. L.; Wang, X. F.; Qian, Q. Y.; Wang, F. B.; Xia, X. H. *ACS Nano* **2009**, *3*, 2653–2659.
(14) Kim, W. S.; Moon, S. Y.; Bang, S. Y.; Choi, B. G.; Ham, H.; Sekino, T.; Shim, K. B. *Appl. Phys. Lett.* **2009**, *95*, 0831031–0831033.
(15) Tuinstra, F.; Koenig, J. L. *J. Chem. Phys.* **1970**, *53*, 1126–1130.
(16) Park, S.; Dikin, D. A.; Nguyen, S. T.; Ruoff, R. S. *J. Phys. Chem. C* **2009**, *113*, 15801–15804.
(17) Jeong, H. K.; Lee, Y. P.; Lahaye, R. J.; Park, M. H.; An, K. H.; Kim, I. J.; Yang, C. W.; Park, C. Y.; Ruoff, R. S.; Lee, Y. H. *J. Am. Chem. Soc.* **2008**, *130*, 1362–1366.
(18) Meyer, J. C.; Geim, A. K.; Katsnelson, M. I.; Novoselov, K. S.; Booth, T. J.; Roth, S. *Nature* **2007**, *446*, 60–63.
(19) Ladislav, K. *Chem. Rev.* **1997**, *97*, 3061–3082.